Desalination and Water Treatment
www.deswater.com

doi: 10.5004/dwt.2022.28958

277 (2022) 144–154
November

Experimental study of phenol removal from aqueous solution by adsorption onto synthesized Faujasite-type Y zeolite

Abderrazek El-Kordy[a], Younes Dehmani[b], Mohamed Douma[a,*], Abdelmjid Bouazizi[a,c], Hajar El Moustansiri[a], Soukaina El Abbadi[a], Najib Tijani[a]

[a]*Materials, Membranes and Nanotechnology Laboratory, BP: 11201 Zitoune, Faculty of Sciences, Moulay Ismail University of Meknès, Meknès, Morocco, emails: m.douma@yahoo.fr (M. Douma), abderrazekelkordy@gmail.com (A. El-Kordy), abdelmjidbouazizi@gmail.com (A. Bouazizi), hajar.elmoustansiri.bcg@gmail.com (H. El Moustansiri), soukainaelabbadi19@gmail.com (S. El Abbadi), najibtij@gmail.com (N. Tijani)*
[b]*Applied Materials and Catalysis, BP. 11201 Zitoune, Faculty of Sciences, Moulay Ismail University of Meknès, Meknès, Morocco, email: dehmaniy@gmail.com*
[c]*Department of Sciences, Ecole Normal Superieure, Moulay Ismail University of Meknès, 50000 Morocco*

Received 14 June 2022; Accepted 27 September 2022

ABSTRACT

This research aims to carry out an experimental study to remove toxic phenol from wastewater by Faujasite-type Y zeolite as adsorbent. The adsorbent was firstly synthetized and characterized by X-ray diffraction to determine both its mineralogical composition and the crystal structure of zeolite, differential thermal analysis-thermogravimetric analysis to understand its thermal behavior with respect to the sintering temperature, the N_2 adsorption/desorption method to get the surface area measurements and scanning electron microscopy coupled with energy-dispersive X-ray spectroscopy to study the surface morphology. The operating conditions such as contact times, pH and temperature of adsorption were studied and optimized to improve efficiently the process of adsorption. The adsorption analysis showed an adsorption capacity of 83 mg/g towards phenol at optimum pH = 4 and 52°C. The reaction kinetics was studied by pseudo-first-order and pseudo-second-order models, and it was observed that the pseudo-second-order accurately described the adsorption kinetics. In addition, the Freundlich and Langmuir adsorption isotherms models were applied, the found results showed that the Langmuir adsorption isotherm model is the most appropriate to describe the adsorption of phenol on Faujasite zeolite. The thermodynamic results also confirm the reversibility and disorder of the process, indicating that the phenol adsorption was primarily physical, and the decisive effect of π–π interactions and H-bonds on the adsorption capacity could not be considered the main force. As well as, high silica zeolites have several acidic sites, and associated base sites, which could act as active adsorption sites for phenol, suggest that the zeolites have potential applications in the removal of organic pollutants from wastewater.

Keywords: Adsorption; Phenol; Faujasite zeolite; Kinetics; Isotherms; Thermodynamics

1. Introduction

Nowadays, the sources of potable water are very limited to fill the daily life needs. Indeed, many parts of the world do not have access to drinking water and urgently need economical, reliable and efficient methods to treat local raw water sources. Additionally, the increase in industrial activities is putting increasing pressure on the world's freshwater reserves [1]. These activities generate a wide variety

* Corresponding author.

Presented at the Second International Symposium on Nanomaterials and Membrane Science for Water, Energy and Environment (SNMS-2021), June 1–2, 2022, Tangier, Morocco

of chemicals that are discharged into the water cycle [2]. Industrial and agricultural discharges containing toxic and/or bio-refractory products have become a major concern, leading to widespread awareness and stricter legislation regarding tolerated limits [3]. Among these pollutants, phenol which is a severe pollutant due to its toxicity. Depending on its duration of exposure, it can cause many diseases even at low concentrations. Phenol is also present in agricultural runoff due to several pesticides affecting soil and groundwater. Phenol reduces soil porosity, affecting seed germination. Therefore, disposing of phenol in a cost-effective and environmentally friendly manner is an effective way to ensure human health and protect the environment.

Despite the continuous improvement of processes and human behavior, the techniques for treating unavoidable pollution still face difficulties because there are no universal treatment methods [4]. Among aqueous effluents, those containing toxic organic pollutants pose specific technological difficulties. Numerous methods and techniques of removal of pollutants have been developed in recent years. Several methods like adsorption, flocculation, oxidation, membrane processes, enzyme degradation, ion exchange, enzyme degradation, etc, have been used to treat phenol-containing wastewater [5].

The adsorption process is a widely used technology for the purification or removal of substances in the gas or liquid phase. Therefore, it is the most favorable method for removing pollutants and has become an analytical method of choice, very effective and simple in its use [6]. In general, it uses materials like highly porous adsorbents or containing functional groups to improve adsorption capacity. Among the used adsorbents, there are clays, activated alumina, activated carbon, agro-industrial residues and natural and synthetic zeolites, etc. [7,8]. Also, several natural and synthetic materials are tested in the adsorption of phenol and can be used in water treatment processes. Zeolitic materials are inorganic crystalline alumina-silicates with an ordered microporous structure and uniform pore size, which present particular physicochemical properties and are useful in various fields (ion exchange, separation and catalysis), due to their controlled porosity and the presence of exchangeable compensation cations, as well as their high hydrothermal resistance [9,10].

The zeolites are among the most studied materials for environmental applications and are a suitable choice as new adsorbents. Especially, FAU-Y zeolite has a larger specific surface area than other types of zeolites with a higher porosity. The main characteristics of this material are: low cost, high stability and well defined pores and a typical microporous structure. In addition, this type of zeolite is very hydrophilic. These properties have made it possible to choose this type of zeolite as an adsorbent support to eliminate phenol in an aqueous medium [11,12].

Structural and textural properties of material depend upon preparation method, used precursors and precipitating agent. Different researchers have widely used this material due to these promising properties in the adsorption of volatile organic compounds [13], trichlorophenol [14,15], CO_2 [16] and Cd(II) [17].

Because of its efficiency, its simplicity of implementation and low capital cost, adsorption remains one of the most widely used techniques for removing organic pollutants. This method requires the choice of an adsorbent with good characteristics (high specific surface area, availability, low cost). Several research works focus on the use of synthetic zeolite in the removal of organic and inorganic pollutants in wastewater [18]. In addition, several reviews show the effectiveness of adsorption on zeolite in the treatment of wastewater [19].

In the present work, low-cost Faujasite-type Y zeolite was hydrothermally prepared and characterized by different techniques. As application to evaluate the material performance, this zeolite was used as an adsorbent of dynamic adsorption experiments to remove phenol from the solution medium. In addition, the adsorption process was systematically studied, including the adsorption kinetics, adsorption isotherms and adsorption thermodynamics.

2. Materials and methods

2.1. Chemicals and reagents

Hydrochloric acid (HCl, 37 wt.%), sodium hydroxide (NaOH, 98 wt.%), sodium aluminate, sodium silicate and polyethylene (PE) were acquired from Sigma-Aldrich for zeolite synthesis. It should be noted that all preparation experiments were performed with self-produced distilled water.

2.2. Adsorbent preparation

2.2.1. Germination gel

To prepare the germination gel, 0.0255 mol of NaOH and 5.328×10^{-3} mol of sodium aluminate were dissolved in 0.277 mol of distilled water. After dissolution, 0.02 mol of sodium silicate were added to the mixture. The polyethylene (PE) container was closed and the gel was allowed to cure for 24 h at room temperature with stirring [20].

2.2.2. Growth gel

The growth gel was prepared as follows: 8.75×10^{-4} mol of NaOH and 0.033 mol of sodium aluminate were dissolved in 1.82 mol of distilled water. After dissolution, 0.125 mol of sodium silicate was added gradually under strong agitation. The gel was left to cure for 2 h after the end of the addition. Once the growth gel was ready, the germination gel was added under strong agitation and the whole was placed in a closed polyethylene (PE) container at 80°C for 24 h. After drying, the zeolite was filtered and washed with distilled water until pH = 10 and finally, it was dried [21].

2.3. Characterization of the adsorbent

The adsorbent was characterized using different techniques. Fourier-transform infrared spectra (FTIR) was collected from 400 to 4,000 cm^{-1} on a FTIR spectrometer (Shimadzu, JASCO 4100). X-ray diffraction analysis is used in order to identify the crystalline phases and it was performed using an X'Pert PRO MPD diffractometer employing CuKα radiation (Kα1 = 1.5418 Å). The surface morphology of the samples was conducted by scanning electron

microscopy (SEM, Topcon Model EM200B), equipped with energy-dispersive X-ray (EDX) analysis. Thermogravimetric analysis (TGA) and differential thermal analysis (DTA) were carried out in an air atmosphere using LABSYS Evo equipment. N_2 adsorption/desorption measurements were obtained using Micromeritics ASAP 2010 to calculate the zeolite textural parameters. The point of zero charges was determined by the potentiometric titration [22].

2.4. Adsorption of phenol

These experiments were done by mixing 20 mL of phenol with a concentration ranging from 10 to 50 mg/L, with a zeolite mass of 0.1 g. The batch experiments on the pH effect were carried out at 298 K. The pH of all solutions was adjusted to the desired pH (of 2 to 11) with a tolerance of ±0.02 from the desired value, under continuous stirring of 400 rpm. The effect of ionic strength on the adsorption equilibrium of zeolite was studied under the following experimental conditions, phenol solutions (10^{-3} M) are mixed with different concentrations of NaCl (0.001, 0.0001 mol/L) and KCl (0.001, 0.0001 mol/L) before the addition of the amount of solid and the continuation of the adsorption process. The experiments on the temperature effect were conducted at temperatures ranging from 20°C to 60°C at pH = 4.

It should be noted that the phenol concentrations were determined at λ = 270 nm, using the Shimadzu UV-1240 spectrophotometer. Eq. (1) was used to determine the adsorption capacity of phenol in the kinetic and isotherm experiments.

$$Q = \frac{C_0 - C_e}{m_{\text{adsorbent}}} \times V_{\text{sol}} \quad (1)$$

where Q is the adsorption capacity (mg/g), C_0 is the initial concentration of the phenol solution (mg/L), C_e is the equilibrium phenol concentration (mg/L), $m_{\text{adsorbent}}$ is the mass of used zeolite (g) and V_{sol} is the volume of the phenol solution (L).

Adsorption experimental data were adjusted to nonlinear kinetic and isotherm models. The modeling of the adsorption kinetics was carried out by the pseudo-first-order and pseudo-second-order according to Eqs. (2) and (3) [23]:

$$q_t = q_q\left(1 - e^{-t \times k_1}\right) \quad (2)$$

$$q_t = q_e^2 \times k_2 \times \frac{t}{q_e \times k_2 \times t + 1} \quad (3)$$

3. Results and discussion

3.1. Characterization of the adsorbent

3.1.1. X-ray diffraction analysis

The X-ray diffractogram of the synthesized zeolite based on silicate and aluminate precursor is given in Fig. 1. It shows that the solid is well crystallized, thus the lines obtained confirm the presence of the crystalline Faujasite-type zeolite phase similar to that reported by Haghdoost et al. [24] (powder diffraction file N° 00-043-0168). The lines of this diffractogram are intense and sharp and no lines other than those of the zeolite phase are detected [25]. The crystal parameters and chemical formula are given in Table 1.

3.1.2. N_2 adsorption/desorption

N_2 adsorption/desorption was used to characterize the pore structure of Faujasite zeolite (Fig. 2). This isotherm

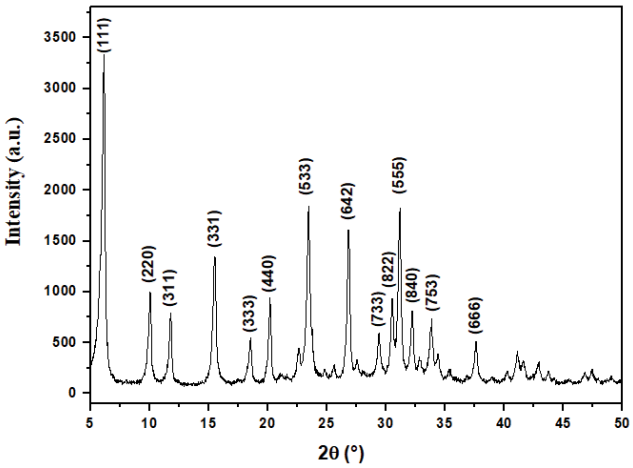

Fig. 1. X-ray diffractogram of Faujasite zeolite.

Table 1
Crystal parameters of the synthesized zeolites

Materials	Parameters	Crystal system	Chemical formula
Zeolite	$a = b = c$ = 24.79 Å α = β = ϰ = 90°	Cubic	$(Na_2)_{3.5}[Al_7Si_7O_{48}]$ 32(H_2O)

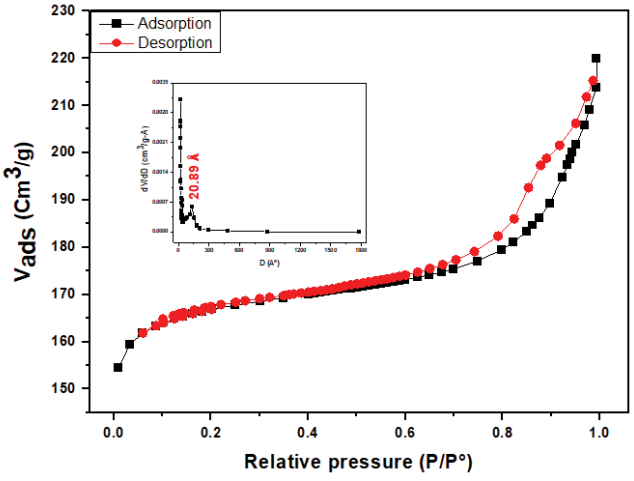

Fig. 2. N_2 adsorption/desorption isotherm of synthesized zeolite and distribution of pore size.

clearly shows an H_4-type hysteresis loop often obtained with rigid stacks of spherical particles of uniform size. The capillary condensation jump is abrupt, signifying homogeneous pore sizes [26]. The textural parameters derived from the nitrogen adsorption isotherms are reported in Table 2 (area, volume and pore diameter).

3.1.3. Fourier-transform infrared spectroscopy

The FTIR of zeolite powder is shown in Fig. 3 and Table 3. The spectra shows bands located at 3,477 and 1,640 cm^{-1}. These bands reflect the presence of elongation and deformation vibrations of the O–H and H–O–H bonds of the adsorbed water molecules, respectively [27,28]. In addition, a strong absorption band located between 1,000 and 1,100 cm^{-1} represents a vibration band of Si–O bond [29]. In addition, two absorption bands at 458 and 553 cm^{-1} are characteristic of the vibration bond of Al–O. Thus, two absorption bands at 687 and 762 cm^{-1} [30] are attributed to the vibrations of the Si–O–Al and Si–O–Si respectively [31].

3.1.4. SEM examination

SEM analysis of the zeolite is presented in Fig. 4. The images show the existence of crystals with an average size ranging from 0.53 to 1.8 μm and a bi-pyramidal shape with a square or cubic octahedral base characteristic of Faujasite-Y type zeolite. The results of the SEM were complemented by chemical analysis by EDX which shows that the synthesized material is a Faujasite type zeolite. The mass percentage of Na, Al and Si is about 51.4 wt.% with that of oxygen (50.8 wt.%) gives an overall percentage equal to 100%, which proves the purity and the best crystallinity of Faujasite [32,33].

Table 2
Structural parameters derived from N_2 adsorption isotherms of Faujasite zeolite

Material	S_{BET} (m^2/g)	V_p (cm^3/g)	D_p (Å)
Zeolite	639.619	0.320	20.894

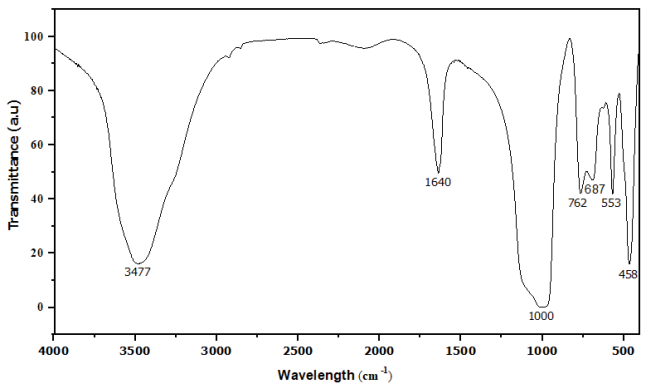

Fig. 3. Infrared spectra of Faujasite zeolite.

3.1.5. Gravimetric and differential thermal analysis

The changes in the physicochemical properties of the zeolite synthesized can be followed by TGA and DTA. The DTA/TGA curves of the Faujasite-type zeolite are shown in Fig. 5. A broad endothermic peak (Fig. 5b) between 25°C and 250°C with a maximum at 160°C associated with a loss of mass (Fig. 5a). It corresponds to the departure of the physisorbed water which does not destroy the crystal structure. The second exothermic peak accompanied by a second loss of mass occurs in the range of 300°C and 500°C and is attributed to the oxidation of zeolite elements (Si and Al) [31–33].

3.1.6. pH of zero charge point

The pH_{pzc} corresponds to the pH value for which the net charge on the adsorbent surface is zero [33]. Results of pH_{pzc} are shown in Fig. 6. The intersection of the curve with the axis passing through zero gives the point of pH of zero charge. The nature of dominant charge on the surface of solid is dependent on the value of pH on comparison with that of the pH_{pzc} = 11.4 of our synthesized material. A negative surface charge in the pH higher than 11.4 and the inverse is correct.

3.2. Adsorption of phenol

3.2.1. pH effect

The pH is an important factor in any adsorption study. It allows to control this process and can condition both the surface charge of the adsorbent as well as the structure of the adsorbate. The results of Fig. 7 show the influence of pH on the adsorption of phenol on zeolite. It should be mentioned that the optimized removal efficiencies are obtained in acidic medium. A better adsorption efficiency was observed at pH equal to 4 by removing phenol with a yield of 98.83%. The observable effect of pH of aqueous solution in the adsorption process can be justified by the relationship between three quantities: pH of the medium, pH of the zero charge point and the dependency of phenols ionization at different pH values. The ionic ratio of phenolate and anionic ions can be calculated by this formula [Eq. (4)].

$$\Phi_{\text{phynolate}} = \frac{1}{\left[1+10^{(pK_a - ph)}\right]} \quad (4)$$

Table 3
Functional groups and assignment of FTIR bands for Faujasite zeolite

Functional groups	Bands (cm^{-1})
O–H stretching vibration	3,477
O–H deformation	1,640
Si–O stretching vibration	1,000–1,100
Si–O–Si stretching vibration	458–553
Si–O–Al bending vibrations	687–762

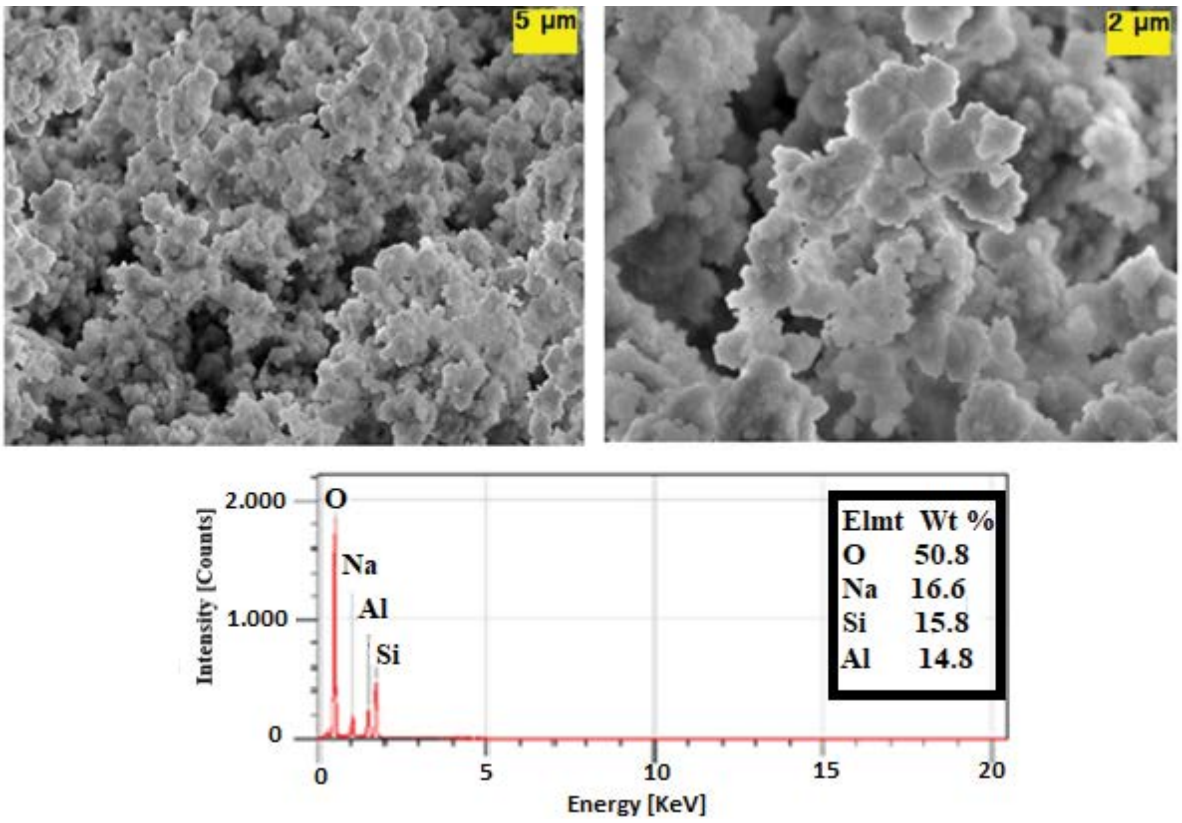

Fig. 4. SEM images and EDX spectra.

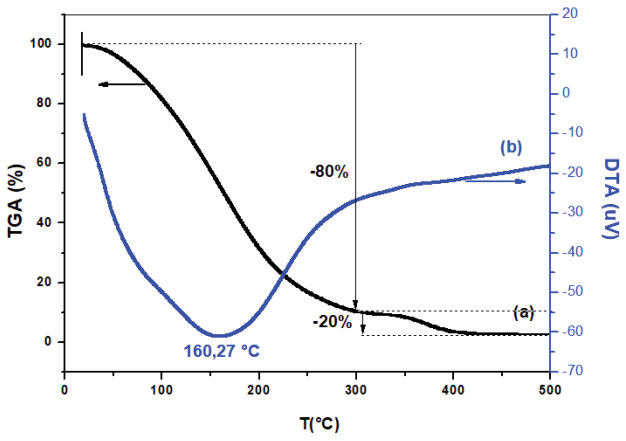

Fig. 5. DTA/TGA curves of Faujasite zeolite.

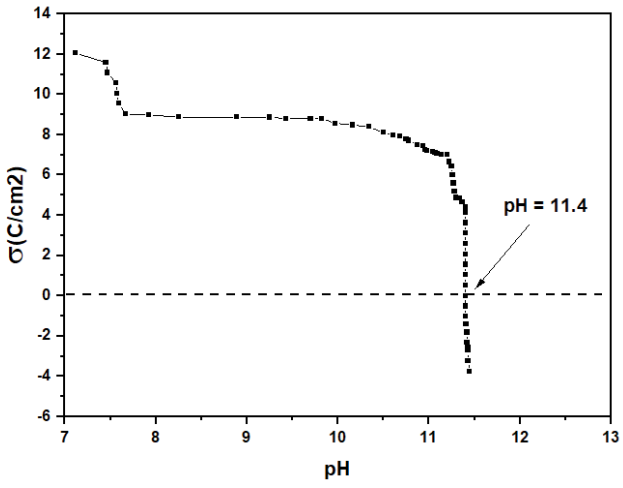

Fig. 6. Surface charge curves of zeolite Faujasite suspensions at ionic strength 0.001 M.

where $\Phi_{phenolate}$ increases as the pH value increased. Table 4 shows the anionic forms at pH 4, 7 and 11 for each studied compound. The amount of phenolic compound adsorbed decreased when the amount of the anionic species in solution increased (i.e., when the pH was increased, being the most optimal conditions at pH = 4). Generally, the modification of the ionic charge of the surface of zeolite is related to the pH value of the medium. The decrease in the quantity adsorbed as a function of pH is due to the presence of electronic repulsion forces between the zeolite surface and the anion formal charge [33].

In other, the pH of the dilution medium conditions the rate of protonation of the compounds. The modification of the ionic charge of the surface of zeolite is related to the pH value of the medium. It is known that below pH of the point of null charge (the point of zero charge of Faujasite-type Y zeolite was 11 and corresponded to the pH on which its surface presented the equilibrium of positive and negative charges) the positive charge that dominates on the surface

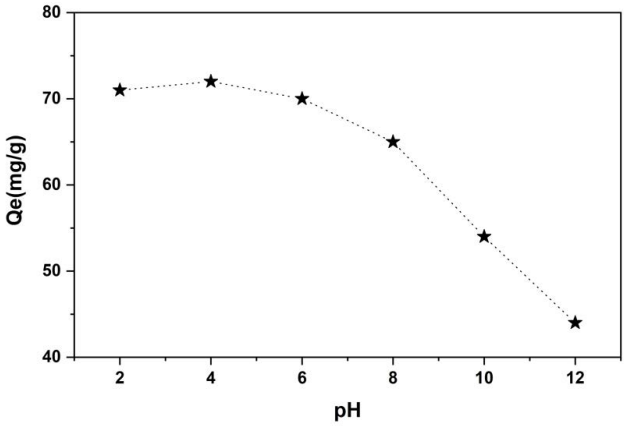

Fig. 7. pH effect on the adsorption of phenol on zeolite.

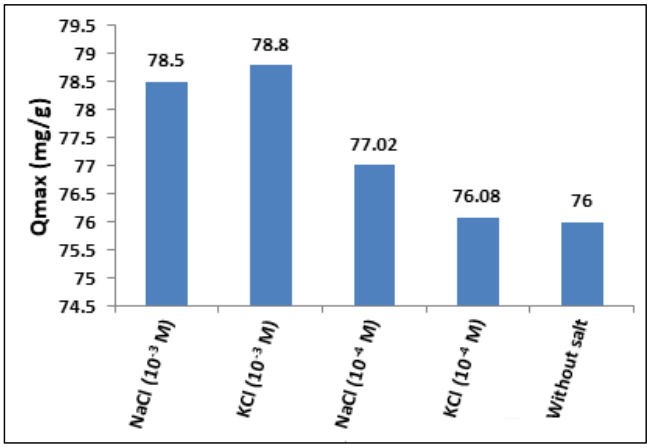

Fig. 8. Effect of ionic strength on the adsorption equilibrium.

Table 4
Ionic forms of phenol at various pH values

Adsorbate	pKa	$\Phi_{phenolate}$		
Phenol	9.95	pH 4	pH 7	pH 11
		1.12×10^{-6}	9.99×10^{-4}	9.09×10^{-1}

of zeolite and pH > pKa of phenol in phenolate form, justifies the important quantity adsorbed of phenol [34]. On the other hand, other authors have suggested the existence of the existence of hydrogen-type bonds between zeolite and phenol thanks to the appearance of hydroxides in the zeolite structure (Mn(OH)*m*). Under these conditions, only non-electrostatic interactions such as π–π interactions and donor-acceptor interactions can promote the adsorption of phenol on the zeolite surface, with a potential contribution from H-bond interactions [35]. These interactions are responsible for the greater adsorption capacity of phenol at acidic pH. In the basic medium, a competition between phenolate ions and hydroxyls (OH^-), in addition to the dominant-negative charge on the surface, justifies the decrease of the adsorbed quantity of phenol [36] can dominate the interaction between phenol and the surface of the zeolite, which explains the strong decrease in the adsorption capacity. It is concluded that the adsorption of phenol is favorable in the acid range, these results are confirmed by works cited in the literature [37–39].

3.2.2. Ionic strength effect

The results obtained in Fig. 8 show that the amount of adsorption increases slightly with the increase of NaCl and KCl concentrations which justifies the role of the charge in the adsorption process of phenol which confirms the presence of electrostatic mechanism. Dong et al. [38] observed the same phenomenon when studying the adsorption of bisphenol A on an exchange-modified zeolite and they suggested that this increase was attributed to the decrease in phenol solubility. Mishra et al. [39] and Yingji et al. [40] observed that with the decrease in phenol solubility, the adsorption decreased, resulting in the clogging of the site by the zeolites.

3.2.3. Temperature effect

Adsorption is a process that can be exothermic or endothermic. For this purpose, we followed the impact of temperature on the adsorption of phenol on zeolite. The effect of temperature on the adsorption of phenol has been studied in numerous works, most of which have noted a positive influence of temperature on the adsorption capacity of zeolites [40]. Since the increase of the temperature facilitates the diffusion of the adsorbed molecules towards the internal pores of the adsorbent particles by decreasing the viscosity of the solution. The most pronounced effect of temperature was observed in the change from 303 to 333 K, the adsorption capacity of phenol was improved from 72 to 84 mg/g (Fig. 9). This significant change in adsorption capacity is due to the mineralogical composition of this zeolite rich in silica which is an expansive mineral under the effect of temperature. This results in a better incorporation of organic molecules in its interfoliar space. The first effect of the temperature increase favors the diffusion of the molecules through the external boundary layer and the internal pores of the adsorbed particles. The second effect of the temperature increase leads to a variation of the spaces between the solid particles and decreases the rate constants of the fixation of the phenol molecules according to the Arrhenius law. Similar behavior to that found in this work has been shown by other works [39].

3.3. Thermodynamic parameter

Parameters such as free energy change (Δ*G*°), enthalpy change (Δ*H*°) and entropy change (Δ*S*°) can be estimated by equilibrium constants changing with temperature (Fig. 10). The free energy change of the adsorption reaction is given by Eq. (5) [41].

$$\Delta G^\circ = -RT \ln K_c \tag{5}$$

where Δ*G*° is the free energy change (kJ/mol), *R* is the gas constant (8.314 J/mol·K), *T* is the absolute temperature (K) and K_C indicates the equilibrium constant (q_e/C_e). The values of Δ*H*° and Δ*S*° can be calculated from the Van't Hoff equation [Eq. (5)] [41].

The values of the thermodynamic adsorption parameters of the pollutant is grouped in Table 5. They show that the adsorption reactions of phenol on zeolite are spontaneous ($\Delta G° < 0$) and endothermic ($\Delta H° > 0$). Also, random interference at the solid–liquid interface was shown by the small positive values of the entropy changes $\Delta S°$ (0.229 kJ/mol·K). The decrease in adsorption free energy values ($\Delta G°$) with temperature indicates that the adsorption of the treated pollutants is promoted by thermal agitation in the range of studied temperatures [42]. It is concluded that the phenol molecules are less organized at the solid/liquid interface than in the liquid phase for these systems. This allows us to conclude that the phenol adsorption process is spontaneous. The results found in this work are in agreement with other previous works which have shown that the adsorption of phenol by zeolites is spontaneous and can be exothermic [43] or endothermic [44].

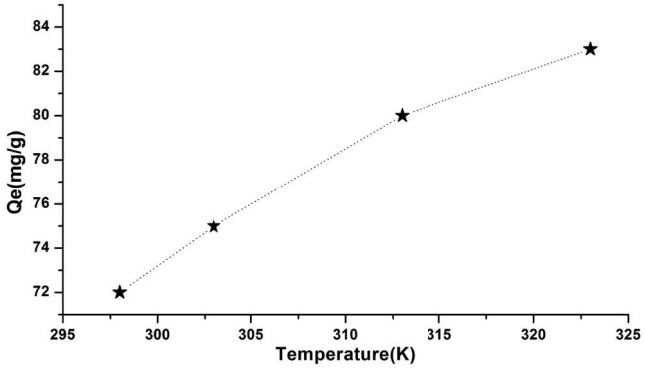

Fig. 9. Effect of temperature on the amount of phenol adsorbed by zeolite.

Table 5
Thermodynamic parameters of phenol adsorption by zeolite

Temperature (K)	$\Delta H°$ (kJ/mol)	$\Delta S°$ (J/mol·K)	$\Delta G°$ (kJ/mol)
298			–4338.07
303	18.69	14.62	–4411.17
313			–4557.37

3.4. Kinetics: contact time effect and modelling

Adsorption experiments to evaluate the effect of contact time on phenol adsorption were performed on phenol solutions with an initial concentration of 50 mg/L and at a temperature of 30°C for a period ranging from 20 to 180 min [42].

The results presented in Fig. 11 show that the adsorbed quantity of phenol increases rapidly in the first 30 min to reach an optimum of 99.46% and remains approximately constant after 30 min, indicating an equilibrium state. This shows that the equilibrium of phenol's adsorption by zeolite is very fast. Then, the adsorption slows down gradually. This is due to the availability of the high number of vacant adsorption sites on the solid surface at the initial stage of adsorption. However, the remaining unoccupied external sites are challenging to occupy as the time is due to the formation of the repulsive force between the phenol molecules on the solid surface (adsorbed) and those in the aqueous phase (free). In addition, the phenol molecules are of medium size and can be quickly diffused into the internal pores until they become saturated, which will reduce the mass transfer between the liquid and solid phase with time [43]. These lead to a decrease in the adsorption rate and a plateau is observed which corresponds to

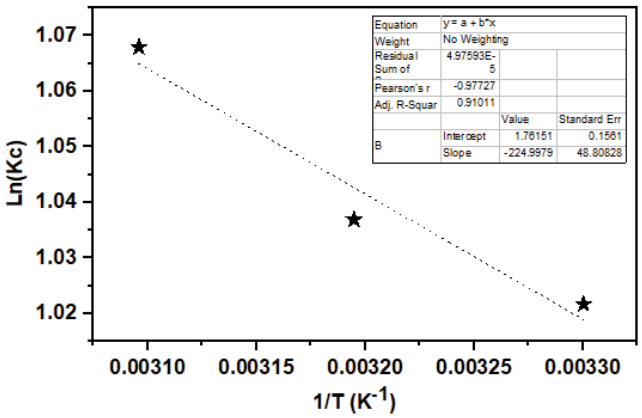

Fig. 10. Variation of $\ln(K_C)$ as a function of $1/T$ (K^{-1}) for the adsorption of phenol on zeolite.

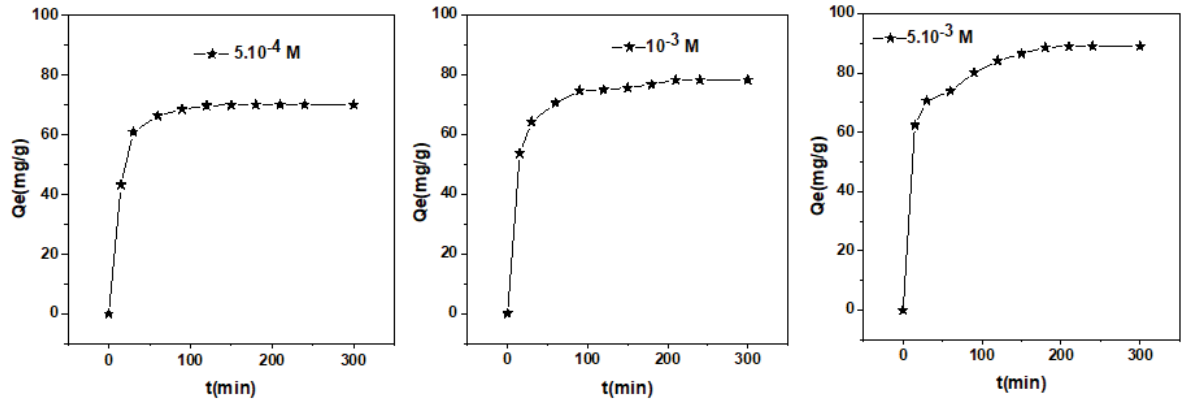

Fig. 11. Variation of the amount of phenol adsorption on zeolite as a function of time.

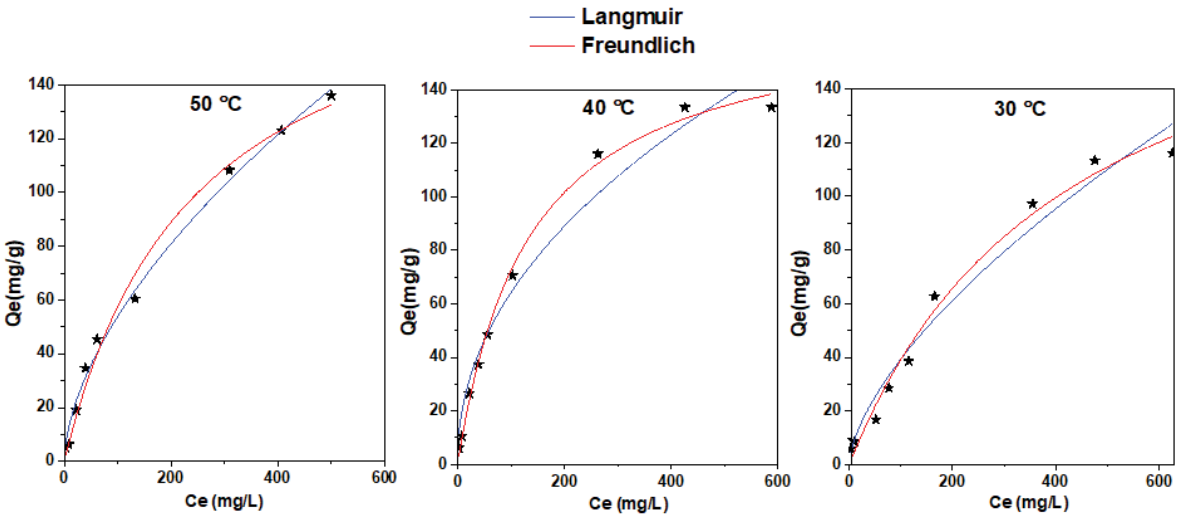

Fig. 12. Adsorption isotherms of phenol on zeolite.

the equilibrium state after 60 min. In short, equilibrium is reached after 30 min for phenol, a strong adsorption of phenol is observed in the first minutes of contact, then the adsorption rate begins to decrease slowly until stabilizing at a maximum limit value at time equilibrium, the quantities retained become invariable, resulting in extremely rapid adsorption. Indeed, 99% of the phenol adsorption capacity is respectively reached during the first minutes.

3.5. Isotherm of phenol adsorption on zeolite

The adsorption isotherms of phenol on zeolite were examined using the Langmuir and Freundlich models (Fig. 12). For the three temperatures studied, the coefficients of correlation (R^2) of the Langmuir models are higher than those obtained with the Freundlich models (Table 6). The model proposed by Langmuir in 1916, is a simple theoretical model whose assumptions are: the adsorption is total when all the sites are covered by a monologue of adsorbed substance, each site can receive a molecule, all the sites are equivalent and the surface is without asperity and the adsorption of a molecule on a site is not influenced by the occupation of the surrounding sites. It can be underlined that in this model, the adsorbent charge tends toward a maximum limit value q_m corresponding to a total occupation of the adsorption sites by a monolayer of the targeted substance [39,43,44].

3.6. Mechanism of adsorption

Three models have been proposed to interpret the adsorption mechanism of phenol [45]. The electron donor-acceptor complex (chemical adsorption), the π–π dispersion interactions (physical adsorption), and the solvent effects. The electron donor-acceptor complex assumes that the surface oxygen groups of zeolite and aromatic rings of phenol act as electron donors and acceptors, respectively [46]. According to the thermodynamic analysis, phenol adsorption was primarily physical, indicating that this mechanism could not be considered the main force.

Table 6
Parameters of the phenol adsorption isotherm on zeolite

Model	Parameters	30°C	40°C	50°C
Langmuir	q_m (mg/g)	170	197	205
	K_L (L/mg)	0.004	0.006	0.002
	R^2	0.98	0.98	0.99
Freundlich	K_F (mg/g)	2,07	7.37	3.60
	$1/n$	0.46	0.63	0.58
	R^2	0.96	0.96	0.99

The solvent effects occur when some adsorption sites for phenol are occupied by water molecules. Water molecules can be adsorbed on the surface oxygen groups by hydrogen bond and block part of pores in zeolite [45]. High-silica zeolites have a high silica content and, therefore, a relatively hydrophobic surface. Phenol is hydrophilic and polar, so phenol is more likely to be adsorbed onto Si–OH single bonds replacing water molecules. High silica zeolites have several acidic sites, and associated base sites, which could act as active adsorption sites for phenol.

The characterization of the solids after adsorption of phenol by FTIR can help to understand the mechanism of adsorption of phenol on zeolite. On the spectra (Fig. 13) we observe the appearance of a band located at 1,030 cm^{-1}. This band is attributed to the vibration of the C–H bond of phenol. Moreover, a remarkable variation of the intensity of the bands according to the concentration of phenol. An important effect on the intensity of the band attributed to the O–H bond which shows the role played by the solvent in this phenomenon. All these elements and the thermodynamic data confirm the fixation and the penetration of phenol molecules in the zeolite and show that the adsorption can be chemical.

3.7. Comparison with other adsorbents

Simplicity, efficiency of the adsorption process and price of the adsorbent are the main factors discussed for its use.

Table 7
Literature results of the adsorption of phenol by different adsorbents

Adsorbent	Adsorption capacity (mg/g)	References
Zeolites Y modified	24	[47]
Magnetic SN-functionalized diatomite	2.04	[48]
Clarified sludge from basic oxygen furnace	1.05	[49]
Hydrotalcite MgAL-CO_3	0.005	[50]
Organo-modified basaltic clay and	41	[51]
NiO	8.52	[52]
Microorganism P. putrid and acid-modified CESEP/ZIF-8	5.96	[53]
Na-bentonite	9.19	[54]
Lignite	6.21	[55]
Moroccan pyrophyllite	11.00	[56]
This work	90	

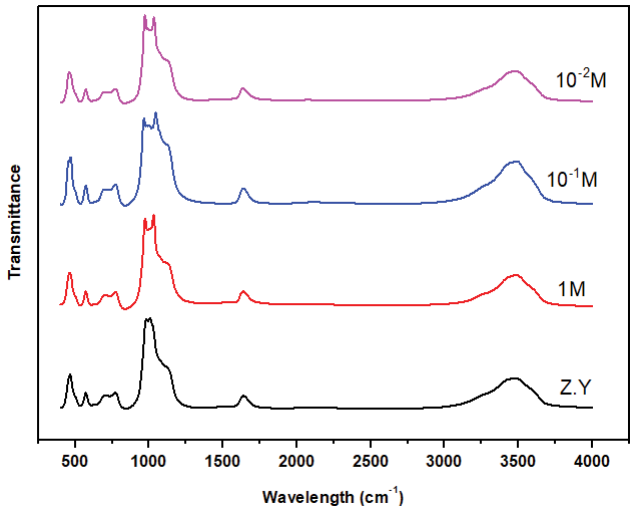

Fig. 13. Infrared spectra of Faujasite zeolite after phenol adsorp

Here, we compared the adsorption capacity of synthetic materials to adsorb phenol in aqueous media with other natural and artificial adsorbents (Table 7). Porous zeolites offer advantages over commercial and a few other adsorbents for phenol removal. To the current end, the table lists the adsorption capacities of economic zeolites with some adsorbents for phenol removal as described within the literature. The reported data show that the adsorption capacity of zeolite for phenol is much higher than that of commercial zeolite and comparatively higher than that of another adsorbent, indicating that the prepared porous zeolite has advantages in the treatment of wastewater containing phenol.

4. Conclusion

In the present work, Faujasite zeolite (FAU) was prepared from sodium aluminate and sodium silicate and characterized by various physicochemical methods. This material was tested as an adsorbent of phenol in aqueous medium. The results of this study show that the zeolite presents excellent adsorption performance of phenol in aqueous solution with a removal efficiency of 98%. The adsorption of phenol on zeolite is affected by temperature and its removal rate increases with increasing temperature and adsorption is favored at acidic pH. The adsorption equilibrium is well represented by the Langmuir isotherm model and the saturation time is fast. Thus, the adsorption kinetics follows a pseudo-second-order kinetic model. Finally all the results show that zeolite has a promising potential to act as an alternative candidate for wastewater treatment.

Acknowledgments

This work was supported by the Ministry of Education and Research in Germany, within the framework of the I-WALAMAR project (01LZ1807C).

References

[1] T. Wang, Y. Wen, B. Lin, Energy consumption and the influencing factors in China: a nonlinear perspective, J. Cleaner Prod., 249 (2020) 119375, doi: 10.1016/j.jclepro.2019.119375.
[2] M.F. Hanafi, N. Sapawe, A review on the water problem associate with organic pollutants derived from phenol, methyl orange, and remazol brilliant blue dyes, Mater. Today:. Proc., 31 (2020) A141–A150.
[3] L. Cui, Y. Wang, X. Han, P. Xu, F. Wang, D. Liu, H. Zhao, Y. Du, Phenolic resin reinforcement: a new strategy for hollow NiCo@C microboxes against electromagnetic pollution, Carbon, 174 (2021) 673–682.
[4] P. Zong, Y. Cheng, S. Wang, L. Wang, Simultaneous removal of Cd(II) and phenol pollutions through magnetic graphene oxide nanocomposites coated polyaniline using low temperature plasma technique, Int. J. Hydrogen Energy, 45 (2020) 20106–20119.
[5] C. Wang, N. Shao, J. Xu, Z. Zhang, Z. Cai, Pollution emission characteristics, distribution of heavy metals, and particle morphologies in a hazardous waste incinerator processing phenolic waste, J. Hazard. Mater., 388 (2019) 121751, doi: 10.1016/j.jhazmat.2019.121751.
[6] A. Dehbi, Y. Dehmani, H. Omari, A. Lammini, K. Elazhari, S. Abouarnadasse, A. Abdallaoui, Comparative study of malachite green and phenol adsorption on synthetic hematite iron oxide nanoparticles (α-Fe_2O_3), Surf. Interfaces, 21 (2020) 100637, doi: 10.1016/j.surfin.2020.100637.
[7] M.T. Nakhjiri, G. Bagheri Marandi, M. Kurdtabar, Preparation of magnetic double network nanocomposite hydrogel for adsorption of phenol and p-nitrophenol from aqueous

solution, J. Environ. Chem. Eng., 9 (2021) 105039, doi: 10.1016/j.jece.2021.105039.
[8] D. Feng, D. Guo, Y. Zhang, S. Sun, Y. Zhao, Q. Shang, H. Sun, J. Wu, H. Tan, Functionalized construction of biochar with hierarchical pore structures and surface O-/N-containing groups for phenol adsorption, Chem. Eng. J., 410 (2021) 127707, doi: 10.1016/j.cej.2020.127707.
[9] M.R. Hossain, M.M. Hasan, N-E-Ashrafi, H. Rahman, M.S. Rahman, F. Ahmed, T. Ferdous, M.A. Hossain, Adsorption behaviour of metronidazole drug molecule on the surface of hydrogenated graphene, boron nitride and boron carbide nanosheets in gaseous and aqueous medium: a comparative DFT and QTAIM insight, Physica E, 126 (2021) 114483, doi: 10.1016/j.physe.2020.114483.
[10] X. Zhang, Z. Song, Y. Dou, Y. Xue, Y. Ji, Y. Tang, M. Hu, Removal difference of Cr(VI) by modified zeolites coated with MgAl and ZnAl-layered double hydroxides: efficiency, factors and mechanism, Colloids Surf., A, 621 (2021) 126583, doi: 10.1016/j.colsurfa.2021.126583.
[11] H. Zhang, Z. Jiang, Q. Xia, D. Zhou, Progress and perspective of enzyme immobilization on zeolite crystal materials, Biochem. Eng. J., 172 (2021) 108033, doi: 10.1016/j.bej.2021.108033.
[12] L. Wang, D.D. Dionysiou, J. Lin, Y. Huang, X. Xie, Removal of humic acid and Cr(VI) from water using ZnO–30N-zeolite, Chemosphere, 279 (2021) 130491, doi: 10.1016/j.chemosphere.2021.130491.
[13] S. Wu, Y. Wang, C. Sun, T. Zhao, J. Zhao, Z. Wang, W. Liu, J. Lu, M. Shi, A. Zhao, L. Bu, Z. Wang, M. Yang, Y. Zhi, Novel preparation of binder-free Y/ZSM-5 zeolite composites for VOCs adsorption, Chem. Eng. J., 417 (2021) 129172, doi: 10.1016/j.cej.2021.129172.
[14] C. Li, J. Chen, J. Wang, Z. Ma, P. Han, Y. Luan, A. Lu, Occurrence of antibiotics in soils and manures from greenhouse vegetable production bases of Beijing, China and an associated risk assessment, Sci. Total Environ., 521–522 (2015) 101–107.
[15] J. Koelmel, M.N.V. Prasad, G. Velvizhi, S.K. Butti, S.V. Mohan, Chapter 15 – Metalliferous Waste in India and Knowledge Explosion in Metal Recovery Techniques and Processes for the Prevention of Pollution, Environmental Materials and Waste: Resource Recovery and Pollution Prevention, Academic Press, 2016, pp. 339–390, doi: 10.1016/B978-0-12-803837-6.00015-9.
[16] M.C. Verbraeken, R. Mennitto, V.M. Georgieva, E.L. Bruce, A.G. Greenaway, P.A. Cox, J.G. Min, S.B. Hong, P.A. Wright, S. Brandani, Understanding CO_2 adsorption in a flexible zeolite through a combination of structural, kinetic and modelling techniques, Sep. Purif. Technol., 256 (2021) 117846, doi: 10.1016/j.seppur.2020.117846.
[17] S. Zhang, T. Lv, Y. Mu, J. Zheng, C. Meng, High adsorption of Cd(II) by modification of synthetic zeolites Y, A and mordenite with thiourea, Chin. J. Chem. Eng., 28 (2020) 3117–3125.
[18] C.D. Johnson, F. Worrall, Novel granular materials with microcrystalline active surfaces-waste water treatment applications of zeolite/vermiculite composites, Water Res., 41 (2007) 2229–2235.
[19] M. Jiménez-Reyes, P.T. Almazán-Sánchez, M. Solache-Ríos, Radioactive waste treatments by using zeolites. A short review, J. Environ. Radioact., 233 (2021) 106610, doi: 10.1016/j.jenvrad.2021.106610.
[20] A. El-Kordy, A. Elgamouz, E.M. Lemdek, N. Tijani, S.S. Alharthi, A.-N. Kawde, I. Shehadi, Preparation of sodalite and Faujasite clay composite membranes and their utilization in the decontamination of dye effluents, Membranes (Basel), 12 (2022) 1–18, doi: 10.3390/membranes12010012.
[21] A. Lahnafi, A. Elgamouz, N. Tijani, I. Shehadi, Hydrothermal synthesis of zeolite A and Y membrane layers on clay flat disc support and their potential use in the decontamination of water polluted with toxic heavy metals, Desal. Water Treat., 182 (2020) 175–186.
[22] H. Ouallal, Y. Dehmani, H. Moussout, L. Messaoudi, M. Azrour, Kinetic, isotherm and mechanism investigations of the removal of phenols from water by raw and calcined clays, Heliyon, 5 (2019) e01616, doi: 10.1016/j.heliyon.2019.e01616.
[23] S.J. Tshemese, W. Mhike, S.M. Tichapondwa, Adsorption of phenol and chromium (VI) from aqueous solution using exfoliated graphite: equilibrium, kinetics and thermodynamic studies, Arabian J. Chem., 14 (2021) 103160, doi: 10.1016/j.arabjc.2021.103160.
[24] F. Haghdoost, S.H. Bahrami, J. Barzin, A. Ghaee, Preparation and characterization of electrospun polyethersulfone/polyvinylpyrrolidone-zeolite core–shell composite nanofibers for creatinine adsorption, Sep. Purif. Technol., 257 (2021) 117881, doi: 10.1016/j.seppur.2020.117881.
[25] J. Jiang, M. Zhu, Y. Liu, Y. Li, T. Gui, N. Hu, F. Zhang, X. Chen, H. Kita, Influences of synthesis conditions on preparation and characterization of Ti-MWW zeolite membrane by secondary hydrothermal synthesis, Microporous Mesoporous Mater., 297 (2020) 110004, doi: 10.1016/j.micromeso.2020.110004.
[26] F. Liu, H. Zhang, Y. Yan, T. Wang, Preparation and characterization of Cu and Mn modified beta zeolite membrane catalysts for toluene combustion, Mater. Chem. Phys., 241 (2020) 122322, doi: 10.1016/j.matchemphys.2019.122322.
[27] M.M. Selim, D.M. EL-Mekkawi, R.M.M. Aboelenin, S.A. Sayed Ahmed, G.M. Mohamed, Preparation and characterization of Na-A zeolite from aluminum scrub and commercial sodium silicate for the removal of Cd^{2+} from water, J. Assoc. Arab Univ. Basic Appl. Sci., 24 (2017) 19–25.
[28] J. Ge, Z. Wu, X. Huang, M. Ding, An effective microwave-assisted synthesis of MOF235 with excellent adsorption of acid chrome blue K, J. Nanomater., 2019 (2019) 4035075, doi: 10.1155/2019/4035075.
[29] J. Zhang, X. Tang, H. Yi, Q. Yu, Y. Zhang, J. Wei, Y. Yuan, Synthesis, characterization and application of Fe-zeolite: a review, Appl. Catal., A, 630 (2022) 118467, doi: 10.1016/j.apcata.2021.118467.
[30] S.L. Hailu, B.U. Nair, M. Redi-Abshiro, I. Diaz, M. Tessema, Preparation and characterization of cationic surfactant modified zeolite adsorbent material for adsorption of organic and inorganic industrial pollutants, J. Environ. Chem. Eng., 5 (2017) 3319–3329.
[31] G. Vezzalini, S. Quartieri, E. Galli, A. Alberti, G. Cruciani, and Å. Kvick, Crystal structure of the zeolite mutinaite, the natural analog of ZSM-5, Zeolites, 19 (1997) 323–325.
[32] Y. Li, G. Zhu, Y. Wang, Y. Chai, C. Liu, Preparation, mechanism and applications of oriented MFI zeolite membranes: a review, Microporous Mesoporous Mater., 312 (2021) 110790, doi: 10.1016/j.micromeso.2020.110790.
[33] X. Wang, A. Chen, B. Chen, L. Wang, Adsorption of phenol and bisphenol A on river sediments: effects of particle size, humic acid, pH and temperature, Ecotoxicol. Environ. Saf., 204 (2020) 111093, doi: 10.1016/j.ecoenv.2020.111093.
[34] J.L.V. Lynch, H. Baykara, M. Cornejo, G. Soriano, N.A. Ulloa, Preparation, characterization, and determination of mechanical and thermal stability of natural zeolite-based foamed geopolymers, Constr. Build. Mater., 172 (2018) 448–456.
[35] Z. Sun, Y. Chen, Q. Ke, Y. Yang, J. Yuan, Photocatalytic degradation of cationic azo dye by TiO_2/bentonite nanocomposite, J. Photochem. Photobiol., A, 149 (2002) 169–174.
[36] Y.F. Hao, L.G. Yan, H.Q. Yu, K. Yang, S.-j. Yu, R.-r. Shan, B. Du, Comparative study on adsorption of basic and acid dyes by hydroxy-aluminum pillared bentonite, J. Mol. Liq., 199 (2014) 202–207.
[37] Q. Li, X. Gao, Y. Liu, G. Wang, Y.-Y. Li, D. Sano, X. Wang, R. Chen, Biochar and GAC intensify anaerobic phenol degradation via distinctive adsorption and conductive properties, J. Hazard. Mater., 405 (2021) 124183, doi: 10.1016/j.jhazmat.2020.124183.
[38] F.X. Dong, L. Yan, X.H. Zhou, S.T. Huang, J.Y. Liang, W.X. Zhang, Z.W. Guo, P.R. Guo, W. Qian, L.J. Kong, W. Chu, Z.H. Diao, Simultaneous adsorption of Cr(VI) and phenol by biochar-based iron oxide composites in water: Performance, kinetics and mechanism, J. Hazard. Mater., 416 (2021) 125930, doi: 10.1016/j.jhazmat.2021.125930.
[39] P. Mishra, K. Singh, U. Dixit, Adsorption, kinetics and thermodynamics of phenol removal by ultrasound-assisted

sulfuric acid-treated pea (*Pisum sativum*) shells, Sustainable Chem. Pharm., 22 (2021) 100491, doi: 10.1016/j.scp.2021.100491.
[40] L. Yingjie, X. Hu, X. Liu, Y. Zhang, Q. Zhao, P. Ning, S. Tian, Adsorption behavior of phenol by reversible surfactant-modified montmorillonite: mechanism, thermodynamics, and regeneration, Chem. Eng. J., 334 (2018) 1214–1221.
[41] M. Keshvardoostchokami, M. Majidi, A. Zamani, B. Liu, Adsorption of phenol on environmentally friendly Fe_3O_4/ chitosan/ zeolitic imidazolate framework-8 nanocomposite: optimization by experimental design methodology, J. Mol. Liq., 323 (2021) 115064, doi: 10.1016/j.molliq.2020.115064.
[42] A. Supong, P.C. Bhomick, R. Karmaker, S.L. Ezung, L. Jamir, U.B. Sinha, D. Sinha, Experimental and theoretical insight into the adsorption of phenol and 2,4-dinitrophenol onto *Tithonia diversifolia* activated carbon, Appl. Surf. Sci., 529 (2020) 147046, doi: 10.1016/j.apsusc.2020.147046.
[43] D.F. Hernández-Barreto, L. Giraldo, J.C. Moreno-Piraján, Dataset on adsorption of phenol onto activated carbons: equilibrium, kinetics and mechanism of adsorption, Data Brief, 32 (2020) 106312, doi: 10.1016/j.dib.2020.106312.
[44] Z. Ghahghaey, M. Hekmati, M. Darvish Ganji, Theoretical investigation of phenol adsorption on functionalized graphene using DFT calculations for effective removal of organic contaminants from wastewater, J. Mol. Liq., 324 (2021) 114777, doi: 10.1016/j.molliq.2020.114777.
[45] H.N. Tran, D.T. Nguyen, G.T. Le, F. Tomul, E.C. Lima, S.H. Woo, A.K. Sarmah, H.Q. Nguyen, P.T. Nguyen, D.D. Nguyen, T.V. Nguyen, S. Vigneswaran, D.-V.N. Vo, H.-P. Chao, Adsorption mechanism of hexavalent chromium onto layered double hydroxides-based adsorbents: a systematic in-depth review, J. Hazard. Mater., 373 (2019) 258–270.
[46] R.I. Yousef, B. El-Eswed, A.H. Al-Muhtaseb, Adsorption characteristics of natural zeolites as solid adsorbents for phenol removal from aqueous solutions: kinetics, mechanism, and thermodynamics studies, Chem. Eng. J., 171 (2011) 1143–1149.
[47] N. Chaouati, A. Soualah, M. Chater, Adsorption of phenol from aqueous solution onto zeolites y modified by silylation, C.R. Chim., 16 (2013) 222–228.
[48] Y. Yu, Z. Hu, Y. Wang, H. Gao, Magnetic SN-functionalized diatomite for effective removals of phenols, Int. J. Miner. Process., 162 (2017) 1–5.
[49] A. Mandal, S.K. Das, Phenol adsorption from wastewater using clarified sludge from basic oxygen furnace, J. Environ. Chem. Eng., 7 (2019) 103259, doi: 10.1016/j.jece.2019.103259.
[50] S. Arhzaf, M.N. Bennani, S. Abouarnadasse, A. Amhoud, Etude de la basicité de l'hydrotalcite MgAL-CO_3 et de son oxyde mixte par adsorption du phénol et par mesure de l'activité catalytique dans la condensation du furfural avec l'acétone, J. Mater. Environ. Sci., 7 (2016) 4226–4236.
[51] S. Richards, A. Bouazza, Phenol adsorption in organo-modified basaltic clay and bentonite, Appl. Clay Sci., 37 (2007) 133–142.
[52] J. Lainé, Y. Foucaud, A. Bonilla-Petriciolet, M. Badawi, Molecular picture of the adsorption of phenol, toluene, carbon dioxide and water on kaolinite basal surfaces, Appl. Surf. Sci., 585 (2022) 152699, doi: 10.1016/j.apsusc.2022.152699.
[53] R. Dong, D. Chen, N. Li, Q. Xu, H. Li, J. He, J. Lu, Removal of phenol from aqueous solution using acid-modified *Pseudomonas putida*-sepiolite/ZIF-8 bio-nanocomposites, Chemosphere, 239 (2020) 124708, doi: 10.1016/j.chemosphere.2019.124708.
[54] H. Asnaoui, Y. Dehmani, M. Khalis, E.K. Hachem, Adsorption of phenol from aqueous solutions by Na–bentonite: kinetic, equilibrium and thermodynamic studies, Int. J. Environ. Anal. Chem., 102 (2022) 3043–3057.
[55] X. Liu, Y. Tu, S. Liu, K. Liu, L. Zhang, G. Li, Z. Xu, Adsorption of ammonia nitrogen and phenol onto the lignite surface: an experimental and molecular dynamics simulation study, J. Hazard. Mater., 416 (2021) 125966, doi: 10.1016/j.jhazmat.2021.125966.
[56] A. El Gaidoumi, A. Chaouni Benabdallah, A. Lahrichi, A. Kherbeche, Adsorption du phénol en milieu aqueux par une pyrophyllite marocaine brute et traitée, J. Mater. Environ. Sci., 6 (2015) 2247–2259.